

Gutzwiller study of extended Hubbard models with fixed boson densities

Takashi Kimura

*Department of Information Sciences, Kanagawa University,
2946 Tsuchiya, Hiratsuka, Kanagawa 259-1293, Japan*

(Dated: February 26, 2019)

We studied all possible ground states, including supersolid (SS) phases and phase separations of hard-core and soft-core extended Bose–Hubbard models with fixed boson densities by using the Gutzwiller variational wave function. We found that the phase diagram of the soft-core model strongly depends on its transfer integral. Furthermore, for a large transfer integral, we showed that a SS phase can be the ground state even below half filling. Finally, we found that the density difference between nearest-neighbor sites, which shows the density order of the SS phase, strongly depends on the boson density, especially for a small transfer integral.

PACS numbers: 03.75.Hh, 05.30.Jp, 05.30.Rt

I. INTRODUCTION

The supersolid (SS) phase that simultaneously exhibits a superfluid (SF) phase and density-wave order has been studied since the first time it was theoretically proposed [1–3]. Although the existence of the SS phase is still a controversial issue, recently, a non-classical moment of inertia of solid ^4He in Vycor glass that suggests the existence of the SS phase has been reported [4].

On the other hand, SS phases may also exist in optical lattices. Cold atoms in optical lattices are new experimental systems where theoretical model Hamiltonians can be more distinctly simulated experimentally without any disorders. For instance, an optical lattice system, as described by a Bose–Hubbard model [5, 6], distinctly showed the phase transition between the SF phase and Mott insulator (MI) [7]. Moreover, recent observations of the long-range dipole-dipole interaction in ^{52}Cr atoms [8] may lead to the realization of the SS phase.

The simplest lattice model with long-range interaction is the extended Bose–Hubbard model with a nearest-neighbor interaction:

$$\begin{aligned}
 H &= H_{kin} + H_{int}^U + H_{int}^V, \\
 H_{kin} &= -t \sum_{\langle i,j \rangle} (a_i^\dagger a_j + a_j^\dagger a_i), \\
 H_{int}^U &= \frac{U}{2} \sum_i n_i(n_i - 1), \\
 H_{int}^V &= V \sum_{\langle i,j \rangle} n_i n_j.
 \end{aligned} \tag{1}$$

Here, t , U , and V are a transfer integral between nearest-neighbor sites, the repulsive intra-site interaction, and the repulsive inter-site interaction between nearest-neighbor sites, respectively. Furthermore, a_i (a_i^\dagger) is the annihilation (creation) operator at site i . In this study, we assume that the lattice is bipartite consisting of sublattices A and B and that the number of nearest-neighbor sites is z .

The extended Bose–Hubbard model which prohibits the multiple boson occupations at one site is called the

hard-core extended Hubbard model, which is equivalent to an XXZ Heisenberg model at half filling ($N = 1/2$, where N is the boson density per site) [9]. The SF order (solid (S) order) of the original Bose–Hubbard model corresponds to the ferromagnetic order in the XY plane and the Ising order along the z axis, respectively, of the mapped XXZ model. On the other hand, the extended Bose–Hubbard model that allows multiple boson occupations at one site is called the soft-core extended Bose–Hubbard model.

Several analytical and numerical methods to study the extended Bose–Hubbard model exist. The strong-coupling perturbation theory [10] has been performed to obtain the phase boundary between the SF phase and the non-SF phase. For the case without any nearest-neighbor interaction [11, 12], this theory determines the phase boundary in perfect agreement with that determined by numerical quantum Monte Carlo (QMC) simulations [13–18]. However, this theory can neither distinguish between the SF and SS phases nor describe discontinuous transitions even if they exist. On the other hand, the mean field (MF) approximation and equivalent Gutzwiller approximations [19, 20] can distinguish between the SF and SS phases and describe discontinuous transitions [21–23], although their validity is limited in high dimensions. If we include a next-nearest-neighbor interaction, both the MF approximation [9, 24–26] for the mapped XXZ model and the previous two-dimensional (2D) QMC studies [26, 27] for the hard-core model away from half filling show that the SS phase with checker-board symmetry can be the ground state. However, later QMC studies [28, 29] have found that the compressibility $\kappa = \frac{dN}{d\mu}$ is negative in the checker-board SS phase, which shows that the checker-board SS phase is unstable against phase separation (PS). The next-nearest-neighbor interaction does not stabilize the checker-board SS phase against the PS, while it stabilizes a striped SS phase as the ground state in a narrow parameter regime.

For the soft-core model, both Gutzwiller [30, 31] and QMC [26, 27] have found stable checker-board SS phases without a next-nearest-neighbor interaction. However, the details of the two studies differ. These Gutzwiller

studies showed stable SS phases both for broad filling and half filling but the PS problem is not a concern in these cases. Contrary to the Gutzwiller studies, these 2D QMC studies [26, 27] did not show the SS phase at half filling and found SS phases away from half filling: however, the system energy is concave below half filling ($N < 1/2$), which suggests a PS instability [26]. A later 2D QMC [32] study more distinctly showed that the SS phase is unstable against PS below half filling by showing the negative compressibility. This situation is similar in one dimension (1D). Both QMC [33, 34] and density-matrix renormalization group (DMRG) [35–37] studies have been performed in 1D. The SS phase was found only above half filling ($N > 1/2$) as in the 2D case but PS did not occur [34, 37].

Contrary to 1D or 2D, a recent three-dimensional (3D) QMC study [38] showed that the SS phase is stable even below half-filling. However, the problem of PS has not been well examined. Hence, to study the problem of the PS below half filling, it is good to not only run numerical simulations but also perform a Gutzwiller analysis which is valid at higher dimensions.

On the other hand, these previous calculations did not directly include the possibility that the system can be separated into two phases. To be more precise, even if we assume the grand canonical ensemble as in QMC studies, we can determine the true boson density by using the Maxwell construction in the separated phase and then estimate the ratio of the SF phase to the solid phase. However, if we start with the canonical ensemble and directly include the possibility that the system can be separated into two phases, we can more distinctly describe the phase diagram with the fixed boson number density of the whole system. Because of long computational time, this framework of calculation may not be easy to perform in exact numerical simulations such as QMC: the reason for such a long computational time is that we minimize the total energy by changing the ratio of the SF or SS phase to the solid phase. However, if we employ a simple approximation for the SF or SS phase such as the Gutzwiller approximation performed in this study, we can distinctly describe the phase diagram which includes the possible PS.

In this work, we study the extended Bose–Hubbard model based on the Gutzwiller approximation. To examine the problem of PS more directly, we have employed the linear programming method [39] to minimize the total energy with a fixed boson number density N of the system. This paper is organized as follows. Section II introduces our calculation method. Sections III and IV present the hard-core and soft-core Bose–Hubbard models, respectively. The paper closes with conclusions from our results in Sec. V. Finally, appendixes explain the details of several perturbative calculations, whose results are compared with the numerical results from the Gutzwiller approximation.

II. CALCULATION METHOD

We employ the following Gutzwiller approximation for the SS and SF phases: $\Psi \equiv \prod_i \Phi_i$. Here, Φ_i is a variational wave function at site i . We assume a bipartite lattice with sublattices A and B and a checker-board symmetry for the SS phase. The variational wave function is assumed to be $\Phi_i = \Phi_{A(B)}$ if the site i belongs to the $A(B)$ sublattice. $\Phi_{A(B)}$ is written as a linear combination of states $|n\rangle$ with n bosons as $\Phi_{A(B)} = \sum_n c_{A(B)n} |n\rangle$. The variational parameters $c_{A(B)n}$ are determined to minimize the energy expectation value. We use the Powell’s method [39] to numerically optimize variational parameters. If the result of the optimization shows $c_{An} \neq c_{Bn}$ and $c_{A(B)n} \neq \delta_{i(j)n}$, the phase is SS; however, if it shows $c_{An} = c_{Bn} \neq \delta_{in}$, the phase is SF (i and j are a non-negative integer and a positive integer, respectively). The first inequality for the SS phase implies the existence of a finite density difference between sublattices A and B , that is, the checker-board symmetric density order. The second inequality implies that the phase is not solid. For the soft-core model, in principle, the sum of n must be taken from $n = 0$ to ∞ ; however, we take the sum from $n = 0$ to $n = 9$, which is sufficient for our calculation for $N \leq 1$. For the hard-core model, by definition, we consider only the two states $|n = 0\rangle$ and $|n = 1\rangle$. The energy expectation value per site is calculated by the Gutzwiller variational wave function as

$$\begin{aligned} E &= \langle H \rangle \\ &= \langle H_{\text{kin}} \rangle + \langle H_{\text{int}}^U \rangle + \langle H_{\text{int}}^V \rangle \\ &= -zt \prod_{i=A,B} \sum_n \sqrt{n+1} c_{in} c_{i(n+1)} \\ &\quad + \frac{U}{4} \sum_{i=A,B} \sum_n n(n-1) |c_{in}|^2 + \frac{zV}{2} N_A N_B. \end{aligned} \quad (2)$$

Here, $N_{A(B)} = \sum_n n |c_{A(B)n}|^2$ is the expectation value of the boson density at the $A(B)$ sublattice. We assume the energy per site of the MI phase with N bosons per site as

$$E_{\text{MI}} = \frac{U}{2} N(N-1) + zVN^2 \quad (3)$$

and that of the solid phase with N_A (N_B) bosons per site on the $A(B)$ sublattice as

$$E_{\text{S}} = \frac{U}{4} \sum_{i=A,B} N_i(N_i-1) + zVN_A N_B, \quad (4)$$

where $N_{A(B)}$ is a non-negative integer. These energies correspond to those obtained from the Gutzwiller variational wave function with $c_{An} = c_{Bn} = \delta_{nN}$ for the MI phase and $c_{An} = \delta_{nN_A}$ and $c_{Bn} = \delta_{nN_B}$ ($N_A \neq N_B$) for the solid phase. Because we neglect surface energy between different phases by supposing the thermodynamic limit, the total energy of the system is

$$E_{\text{tot}} = \sum_i \gamma_i E_i \quad (5)$$

for the boson number condition

$$N_{\text{tot}} = \sum_i \gamma_i N_i. \quad (6)$$

Here, $\{E_i\}$ and $\{N_i\}$ (where $i = \text{SF}, \text{SS}, \text{MI}$, and solid) are the energies and boson number densities, respectively, of all possible phases and $\{\gamma_i\}$ are the ratio of areas or volumes of the phase i in the whole system. For the linear programming method [39], we must minimize E_{tot} as a function $\{\gamma_i\}$. Only one γ_i (corresponding to the uniform phase) or two γ_i s (corresponding to the PS) can be nonzero as a result of minimizing E_{tot} because there is only one additional condition: the boson number condition. In our calculation, we optimize the sets of N_{SS} and N_{SF} , which give E_{SS} and E_{SF} , respectively, in order to find the $\{\gamma_i\}$ that minimizes E_{tot} . For simplicity, however, we neglected the possibility of the separated phase that splits into the SF and SS phases that is highly unlikely.

In more detail, in order to obtain $E_{\text{SF(SS)}}$ for a given $N_{\text{SF(SS)}}$, we add a term to the Hamiltonian $\beta(N - N_{\text{SF(SS)}})^2$, where β is a large positive value and is an additional variational parameter for minimizing the total energy. Minimizing the expectation value of $H + \beta(N - N_{\text{SF(SS)}})^2$, we obtain a SF phase with a given $N_{\text{SF(SS)}}$ without the direct boson number condition $\sum_n n |c(n)|^2 = N_{\text{SF(SS)}}$ [40]. Because $N_{\text{new}} = \sum_n n |c(n)|^2$ is slightly different from the original $N_{\text{SF(SS)}}$ as a result of the minimization, we adopt N_{new} as the boson density. By changing $N_{\text{SF(SS)}}$, which gives N_{new} and $E_{\text{SF(SS)}} = \langle H \rangle$, we finally obtain the minimized E_{tot} and the corresponding phases and their ratios $\{\gamma_i\}$.

III. THE HARD-CORE MODEL

In the hard-core extended Hubbard model, we prohibit multiple occupations at a site and define the Gutzwiller variational wave function as

$$\Phi_{A(B)} = c_{A(B)0}|0\rangle + c_{A(B)1}|1\rangle. \quad (7)$$

At half filling ($N = 1/2$), $|c_{A(B)0}|^2 + |c_{A(B)1}|^2 = 1$ from the normalization condition, and $|c_{A1}|^2 + |c_{B1}|^2 = 1$ from the boson number condition. If we set $x = c_{A0}$, then $c_{A1} = c_{B0} = \sqrt{1-x^2}$ and $c_{B1} = x$. Hence, the system energy per site is

$$\begin{aligned} E &= -zt c_{A0} c_{A1} c_{B1} c_{B1} + \frac{zV}{2} |c_{A1}|^2 |c_{B1}|^2 \\ &= \left(-zt + \frac{zV}{2} \right) \left[\left(x^2 - \frac{1}{2} \right)^2 - \frac{1}{4} \right]. \end{aligned} \quad (8)$$

If $V > 2t$, then $x^2 = 0$ or 1 and the phase is solid with $N_A = 1$ and $N_B = 0$ (assuming $N_A \geq N_B$ without any loss of generality); however, if $V < 2t$, then $x^2 = \frac{1}{2}$ and the phase is SF. Hence, the SF–S phase transition occurs at $V = 2t$ and is discontinuous. This result agrees with those of previous papers [25, 41]

Away from half filling, we can obtain the SF–SS phase boundary by a perturbative calculation setting $c_{A(B)n} = c_n + \delta c_{A(B)n}$, where $\delta c_{A(B)n}$ are the infinitesimal quantities (see Appendix A.1 for details). The result is

$$V_C = t \frac{N^2 + (1-N)^2}{N(1-N)}. \quad (9)$$

Namely, the energy of the SS phase is lower (higher) than that of the SF phase for $V > V_C$ ($V < V_C$). V_C^{SS} is invariant under $N \rightarrow 1 - N$ because of the particle-hole symmetry of the hard-core model. Equation 9 agrees with the previous MF result if the next-nearest-neighbor interaction (which is needed to stabilize the SS phase in the grand canonical ensemble) is zero (see. Eq. 6 of Ref. [26]). However, 2D QMC calculations [28, 29] show that the SS phase is not stable against PS, as explained in Sec. I.

To study the PS from the SF phase into the SF phase and the solid (MI) phase, we set the ratio of the solid (MI) phase as γ_{SM} . When the total boson density is N , the number density condition near the SF–PS phase boundary is written as

$$(1 - \gamma_{\text{SM}})(N - \delta N) + \gamma_{\text{SM}} N_{\text{SM}} = N. \quad (10)$$

Hence,

$$\delta N \simeq (N_{\text{SM}} - N) \gamma_{\text{SM}}. \quad (11)$$

Here, $N - \delta N$ ($\delta N \ll N$) is the number density of the SF phase and $N_{\text{SM}} = 1/2$ ($N_{\text{SM}} = 1$), if the other phase is the solid (MI) phase. The system energy per site is

$$\begin{aligned} E &= \gamma_{\text{SM}} E_{\text{SM}} + (1 - \gamma_{\text{SM}}) E_{\text{SF}}, \\ E_{\text{SF}} &= -zt |c_0|^2 |c_1|^2 + \frac{zV}{2} |c_1|^4 \\ &= -zt(1 - N + \delta N)(N - \delta N) \\ &\quad + \frac{zV}{2} (N - \delta N)^2. \end{aligned} \quad (12)$$

Here, E_{SF} is the energy of the SF phase and E_{SM} is that of the solid or the MI phase: $E_{\text{SM}} = 0$ for the solid phase, and $E_{\text{SM}} = zV/2$ for the MI phase. Equating the coefficient of γ_{SM} (or δN) to zero, we obtain the phase boundary between the SF phase and the separated phase that splits into the SF and the solid phases [PS(SF+S) phase]. Interestingly, the critical value of V is found to be the same as that obtained from Eq. 9. On the other hand, the separated phase that splits into the SF and the MI phases cannot occur (see Appendix A.2 for details). Hence, the calculations cannot determine the ground state for $V > V_C$. Therefore, to determine the ground state for $V > V_C$, we numerically examined the phase diagram by optimizing the Gutzwiller variational wave function; we found that the ground state for $V > V_C$ is the PS(SF+S) phase (Fig. 1). There is no stable SS phase, which agrees with the 2D QMC calculations [28, 29]. The phase boundary agrees with V_C within the

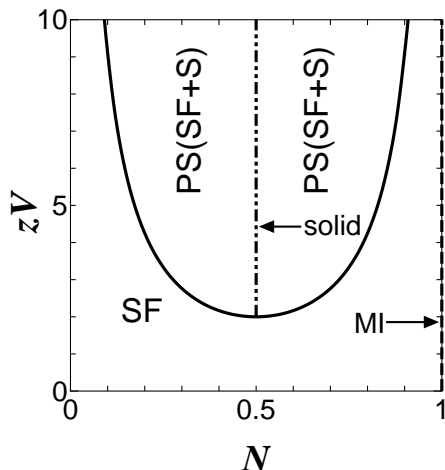


FIG. 1: Phase diagram of the hard-core model. The phase PS(SF+S) means the separated phase that splits into the SF and solid phases. The two-dot dashed curve at half-filling shows the solid phase and the dashed curve at unit-filling shows the MI phase.

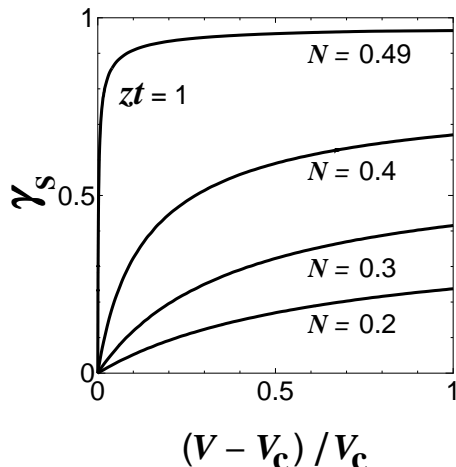


FIG. 2: Interaction dependence of γ_S [the weight of the solid phase in the PS(SF+S) phase]. V_C is the critical value at the SF-PS(SF+S) transition at each value of zt ($zV_C = 4.250, 2.762, 2.167, 2.002$ for $zt = 0.2, 0.3, 0.4, 0.49$, respectively).

numerical error and the phase transition is continuous as the perturbative calculation assumed. We also confirmed that the variational parameter γ_{SM} is finite when $V > V_C$ (Fig. 2). The results for boson density N are in exact agreement with those obtained for the boson density $1 - N$ because of the particle-hole symmetry. The closer N approaches to $1/2$, the faster γ_{SM} increases as a function of $(V - V_C)/V_C$, which reflects the discontinuous SF-S phase transition at half filling.

IV. THE SOFT-CORE MODEL

In this section, we study the soft-core extended Hubbard model. We employ the Gutzwiller variational wave function and numerically optimize its variational parameters, which we hereafter call “the full numerical calculation(s).” We also perform perturbative calculations that limit the Hilbert space of the Gutzwiller variational wave function and partly include numerical calculations. We compare these perturbative calculations with the full numerical calculations. In subsection A, the half-filled case is examined, and the SS phase exists in between the SF phase for small zV/U and the solid phase for large zV/U . In subsection B, the non half-filled case is examined, and we show that the phase diagram on the $zV/U - N$ plane changes qualitatively from small zt/U to large zt/U . As for the figures in this section, solid curves represent results obtained by the full numerical calculations (unless otherwise noted); in addition, dashed curves represent the phase boundaries if the full numerical calculations show that the phase transitions are discontinuous.

A. HALF FILLING

Let us begin with the half-filled ($N = 1/2$) case. Previous 2D QMC calculations [26, 27] showed that there is no SS phase at half filling and that the SF phase at the small nearest-neighbor interaction zV/U directly transits to the solid phase as the nearest-neighbor interaction zV/U increases. On the other hand, for 3D calculations, where the MF approach (such as that used in the present study) may be valid, the existence of the SS phase at half filling remains an unanswered question. Previous studies using the Gutzwiller variational wave function showed that the SS phase may exist at half filling. However, the PS problem has not yet been studied.

To examine whether the SS phase can exist at half filling, we must compare the critical nearest-neighbor interaction of the SS-solid transition with that of the SF-SS transition. To analytically study the SS-solid phase boundary, we set $c_{A0} = \delta\alpha_0$, $c_{A1} = 1 - \delta\alpha_1$, and $c_{A2} = \delta\alpha_2$ for sublattice A, $c_{B0} = 1 - \delta\beta_0$, $c_{B1} = \delta\beta_1$, and $c_{B2} = \delta\beta_2$ for sublattice B in the Gutzwiller variational wave function. Here, $\delta\alpha_n$ and $\delta\beta_n$ ($n = 0, 1, 2$) are infinitesimal quantities and when all of them are zero, the phase is solid. By expanding the total energy in terms of $\delta\alpha_n$ and $\delta\beta_n$, we obtain the critical nearest-neighbor interaction V_C as a power-law expansion of zt/U :

$$zV_C^{\text{SS-S}} = 2zt + 2\frac{z^2t^2}{U} + 2\frac{z^3t^3}{U^2} + O\left(\frac{z^4t^4}{U^3}\right) \quad (13)$$

(see for Appendix B.1 for details).

To analytically study the SF-SS phase transition, we limit the Hilbert space of the Gutzwiller variational wave function to three states: $|0\rangle$, $|1\rangle$, and $|2\rangle$. Further, we set $c_{Ai} = c_n + \delta\alpha_n$ and $c_{Bi} = c_n + \delta\beta_n$ ($\delta\alpha_n \neq \delta\beta_n$), [where

$\delta\alpha_n$ and $\delta\beta_n$ ($i = 0, 1, 2$) are infinitesimal quantities]. Then, when $\delta\alpha_n = \delta\beta_n = 0$, the phase is the SF. This approximation is valid when zt/U is small, because the states with many bosons are neglected in the Gutzwiller variational wave function. By expanding the total energy in terms of $\delta\alpha_n$ and $\delta\beta_n$, the critical nearest-neighbor interaction is obtained as

$$zV_C^{\text{SF-SS}} = 2zt + 2\frac{z^2t^2}{U} + O\left(\frac{z^4t^4}{U^3}\right) \quad (14)$$

(see for Appendix B.2 for details). Because a term of the order of $\frac{z^3t^3}{U^2}$ is absent in $V_C^{\text{SF-SS}}$, $V_C^{\text{SF-SS}} < V_C^{\text{SS-S}}$ and the SS phase is possible for intermediate V satisfying $V_C^{\text{SF-SS}} < V < V_C^{\text{SS-S}}$.

We numerically verify these results. Figure 3 shows the phase boundaries obtained by the perturbative calculations (dashed and dot-dashed curves) and by the full numerical calculations (solid curves). This figure shows a stable SS phase between the SF phase and the solid phase. As expected, both the SS-solid and SF-SS phase boundaries determined by perturbative calculations are in good agreement with those determined by full numerical calculations (especially in small zt/U). Figure 4 shows the interaction dependence of the density difference between sublattices A and B $\delta n = |N_A - N_B|$, which shows the density wave order of the SS phase. Here, $zV_C = zV_C^{\text{SF-SS}}$ is the critical value for the SF-SS transition at each value of zt/U . The phase transition is continuous and δn changes more rapidly for smaller zt/U . However, the phase transition is continuous in the soft-core model under the influence of the finite weights of the high boson number ($n \geq 2$) states in the SF or SS phase. The width of ΔV for the SS phase is very small ($2z^2t^3/U^2$) for small zt/U . Therefore, it might be difficult to find the SS phase at half filling with numerical simulations, and if it does exist, a large zt/U is needed to find it.

B. AWAY FROM HALF FILLING

Let us start by analyzing the phase diagram for a small transfer integral zt/U . Figure 5(a) shows the phase diagram for a small zt/U of 0.03. This phase diagram is similar to that of the hard-core model. Namely, the upper bound of zV/U for the SF phase has a minimum value near the half filling, which is similar to that of the hard-core model with the particle-hole symmetry. The phase separation occurs for large zV/U below the half filling, and the separated phase is the PS(SF+S) phase as in the hard-core model. However, the SS phase appears above the half filling. These properties agree with those from a 2D QMC study with $zt/U = 0.08$ [32]. On comparing with the results from the full numerical calculations, we calculate the results from the following three perturbative equations for the phase boundary: perturbation 1 is Eq. 9 and it is the same as that used in Sec. III, perturbation 2 is Eq. B16 and it gives the SF-SS phase

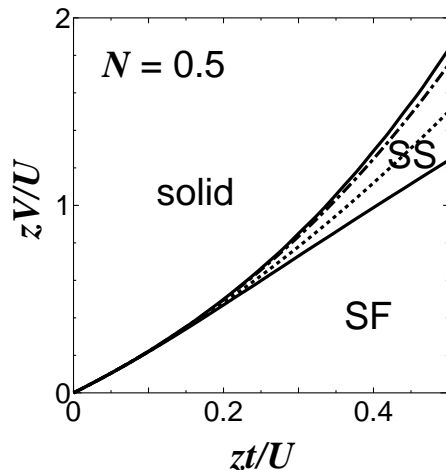


FIG. 3: Phase diagram of the soft-core model at half filling. Solid curves represent the SF-SS and SS-solid phase boundaries. The dashed (dot-dashed) curve represents the SF-SS (SS-solid) phase boundary obtained from Eq. 14 (Eq. 13).

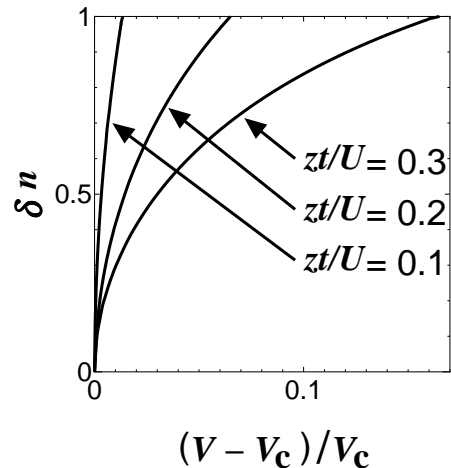


FIG. 4: Interaction dependence of the density difference between sublattices A and B $\delta n = |N_A - N_B|$ in the SS phase of the soft-core model at half filling. V_c is the critical value at the SF-SS transition at each value of zt/U ($zV_C/U = 0.219, 0.469, 0.730$ for $zt/U = 0.1, 0.2, 0.3$, respectively).

boundary, and perturbation 3 is Eq. B24 and it gives the SF-PS(SF+S) phase boundary. For perturbation 2 and 3, we employ a limited Hilbert space with $|N = i\rangle$ where $i = 0, 1, 2$ (see Appendixes B.2 and B.3 for details). For perturbation 3, we have to assume the fixed boson number for the solid phase: we assume $N_A = 1$ and $N_B = 0$ in Fig 5(a) and 5(b). Because perturbation 1 uses the Hilbert space with $|N = i\rangle$ for i only 0 or 1, in principle, perturbations 2 and 3 should be better than perturbation 1. However, perturbations 2 and 3 require a numerical calculation to minimize the SF energy in the limited Hilbert space. Figure 5(a) plots the result of the perturbation 1 (dot-dashed curve), and it is in

almost perfect agreement with the full numerical calculation (solid curve), except for large N where the SF-SS phase boundary disappears [also see Fig. 5(b), which enlarges Fig. 5(a) around $zV/U = 1$]. Perturbations 2 and 3 give almost the same results as those of perturbation 1; therefore, they also agree almost exactly with the full numerical calculations, except for large N .

Figure 5(b) shows that PS also appears above half filling but the region is very small compared to that obtained by the 2D QMC [32]. There are also two PSs for $0.55 < N < 1.0$: one splits into the SS and solid phases [PS(SS+S) phase], and the other splits into the SF and the solid phases [PS(SF+S)]. The PS(SS+S) phase is sandwiched between two SS phases. The solid phases in both separated phases have $N_A = 2$ and $N_B = 0$.

Figure 6 confirms the existence of SS phase above half filling in the soft-core model. Here, the critical values of nearest-neighbor interaction V_C for the SF-SS transition (solid curves) and for the artificial SF-PS(SF+S) transition (dashed curves) are shown for small zt/U . The artificial SF-PS(SF+S) transition was obtained by setting the variational parameter of the Gutzwiller variational wave function as $c_{An} = c_{Bn}$. Because V_C for the SF-SS transition is always smaller than that for the SF-PS(SF+S) transition, the SS phase overcomes the PS(SF+S) phase above half filling for small but finite zt . Further, the difference between V_C for the SF-SS transition and the SF-PS(SF+S) transition disappears in the limit of $zt/U \rightarrow 0$ that corresponds to the hard-core limit where the two phase boundaries coincide as discussed in Sec. III.

The nearest-neighbor interaction dependence of $\delta n = |N_A - N_B|$ is also of interest [see Fig. 7(a) and Fig. 7(b), which enlarges Fig. 7(a) around $1.001 \leq zV/U \leq 1.002$]. Note that δn has a discontinuity at $zV_C/U \simeq 1.001$. The SS phase has small δn for $zV/U \leq 1$, whereas it has large $\delta n \simeq 2N$ ($N_A \simeq 2N$ and $N_B \simeq 0$) for $zV/U > 1.002$ after a rapid increase of δn in a narrow PS(SS+S) region ($1.001 \leq zV/U \leq 1.002$), where the curves of δn for different N are almost indistinguishable [see Fig. 7(b)]. Because $\delta n \simeq 2N$, δn is larger for larger N for $zV/U > 1.002$. Contrarily, δn is smaller for larger N for $zV/U \leq 1.001$, reflecting that the critical value of zV/U for the SF-SS transition is an increasing function of N above half filling.

Figures 8(a) and 8(b) show the phase diagram for an intermediate $zt/U = 0.3$, where the PS region above half filling exists but again is very small. The phase diagram departs from the particle-hole symmetric one. The SS phase below half filling appears in an intermediate zV in agreement with Gutzwiller [30, 31] and 3D QMC [38] calculations (with $zt/U = 0.33$) for the grand canonical ensemble. The results from the perturbative calculations (dot-dashed curves) are in good agreement with those from the full numerical calculations (solid curves): perturbation 3 is in almost perfect agreement with the SF-PS(SF+S) phase boundary, and perturbation 2 is also in excellent agreement with the SF-SS phase boundary, except for the large $N \sim 1$ region where the SF-SS tran-

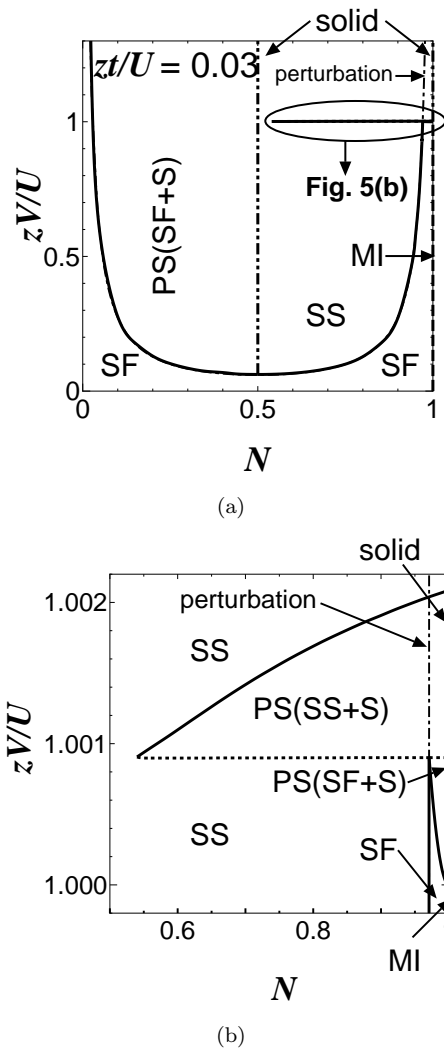


FIG. 5: Phase diagram of the soft-core model for $zt/U = 0.03$. Figure 5(a) shows the whole phase diagram. The solid curve shows the SF-PS(SF+S) or SF-SS phase boundary. The dot-dashed curve for the SF-SS phase boundary obtained by the perturbative calculation Eq. 9 cannot be distinguished from the solid curve, except for large N where the SF-SS transition curve disappears. Figure 5(b) enlarges Fig. 5(a) around $zV/U = 1$ and $N = 1$. Here, the solid (dashed) curves for the phase boundaries show phase transitions that are continuous (discontinuous). The separated phase that splits into the SS and solid phases [PS(SS+S) phase] is sandwiched between two SS phases. In both Figs. 5(a) and 5(b), the two-dot-dashed lines at half filling or unit filling show the solid phase, and the long-dashed line at unit filling shows the MI phase.

sition becomes discontinuous, and thus, cannot be described by the perturbative calculation.

Figure 8(b) enlarges Fig. 8(a) around $zV/U = 1.1$ and $N \sim 1$, where we find a small PS(SF+S) phase. The curve of perturbation 3 in Fig. 8(b) is calculated assuming a solid phase with $N_A = 2$ and $N_B = 0$, while that in Fig. 8(a) is calculated assuming the solid phase $N_A = 1$ and $N_B = 0$ as in Fig. 5(a) and 5(b). In Fig. 8(b),

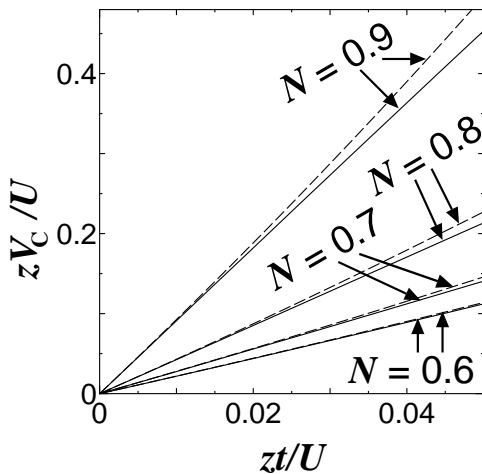


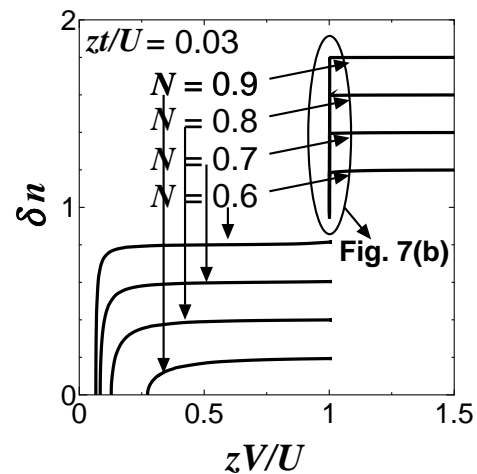
FIG. 6: Critical nearest-neighbor interaction V_C for the SF-SS transition (solid curves) and for the artificial SF-PS(SF+S) transition (dashed curves) above half filling. Note that there are also solid and dashed curves for $N = 0.6$, although the distance between them is very small.

the curve of perturbation 2 far from the results obtained by full numerical calculations; however, the difference is indeed at most about 1% [it only appears large because Fig. 8(b) is an enlarged view].

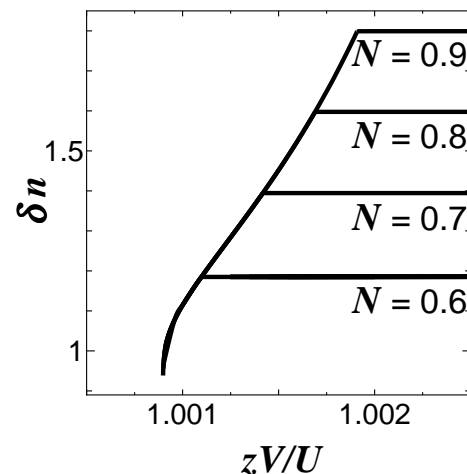
Figure 9 shows the nearest-neighbor interaction dependence of δn above half filling for $zt/U = 0.3$. As in Fig. 7, δn is larger for larger N for large zV/U and $\delta n \simeq 2N$, whereas δn is smaller for larger N for small zV/U . However, contrary to the case of $zt/U = 0.03$, δn shows no discontinuity and the two curves of δn for two different N s intersect around $zV/U \simeq 1.1$. Note that the crossing points of the two curves of δn for two different N s are not the same, and they depend on the pair of N s, although they are close to each other.

Figure 10 shows the nearest-neighbor interaction dependences of δn and γ_S of the soft-core model for $zt/U = 0.3$ below half-filling in the SS phase and PS(SF+S) phases, respectively. This shows that the SS-PS(SF+S) transition is discontinuous. For $N = 0.3, 0.35$, and 0.4 , γ_S (δn) is zero below (above) the critical value of zV/U for the SF-PS(SF+S) transition and discontinuously becomes finite above (below) the phase transition. For $N = 0.25$, δn is zero in the entire figure because the SS phase does not exist.

Figure 11 shows the phase diagram for a large $zt/U = 1$. Only the SF and SS phases exist and there are no phase separations. The SF-SS transition is continuous throughout the figure. The critical zV/U in between these phases is a decreasing function of the boson density N . This may be explained as follows: for large zt/U , the ratio t to V is the only important factor determining the phase (SF or SS, not the PS), because the lattice does not play an important role, except for half or unit filling, and N merely affects the SF-SS phase boundary (V more strongly affects the phase for larger N). The dot-dashed



(a)

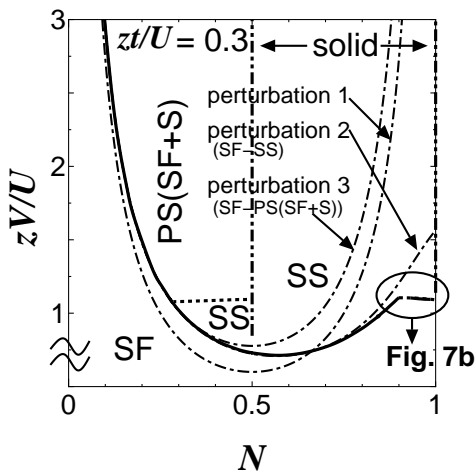


(b)

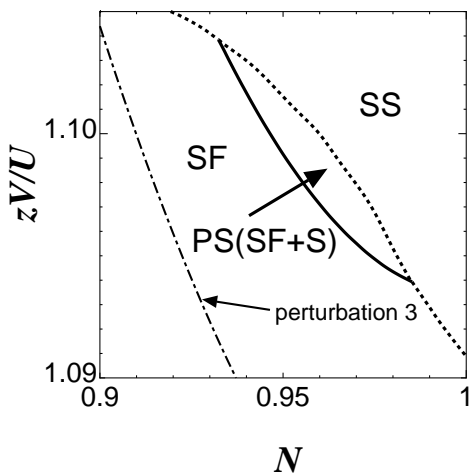
FIG. 7: Nearest-neighbor interaction dependence of $\delta n = |N_A - N_B|$ in the SS phase of the soft-core model for $zt/U = 0.03$. δn is larger at smaller N for $zt/U \leq 1.000$, is discontinuous at $zV_C/U \simeq 1.001$, and smaller at smaller N for $zt/U \geq 1.002$. Figure 7(b) enlarges Fig. 7(a) around the PS(SS+S) phase ($1.001 \leq zV_C/U < 1.002$). In the PS(SS+S) phase, δn is a sharp increasing function of zV/U , and the curves of δn for different N coincide.

curve of perturbation 1 does not agree with the full numerical calculation (solid curve) because the perturbation 1 shows the particle-hole symmetry of the hard-core model, which is distinctly broken here. However, the dot-dashed curve of perturbation 2 is in excellent agreement with the solid curve, except for large N .

Figure 12 shows the nearest-neighbor interaction dependence of δn in the SS phase of the soft-core model for $zt/U = 1$. δn is larger for smaller N at the same zV/U because the critical value of zV for the SF-SS transition is smaller for larger N (Fig. 11). Contrary to the case of $zt/U = 0.03$ (Fig. 6) or $zt/U = 0.3$ (Fig. 9), δn is a smooth increasing function of N and zV/U , and the two curves of δn for two different N no longer intersect.



(a)



(b)

FIG. 8: Phase diagrams of the soft-core model for $zt/U = 0.3$. Figure 8(a) shows the whole phase diagram. The solid curve shows the SF-PS(SF+S) or SF-SS transition. The dot-dashed curves are the perturbative results Eq. 9 (perturbation 1), Eq. B16 (perturbation 2), and Eq. B24 (perturbation 3). The two-dot-dashed lines at half filling and unit filling represent the solid phase. Figure 8(b) enlarges Fig. 8(a) around $zV/U = 1$ and $N = 1$. Here, the solid curve shows the continuous SF-PS(SF+S) phase transition, and the dashed curve shows the discontinuous SF-SS and PS(SF+S)-SS phase transition.

V. CONCLUSION

In this work, we studied the hard-core and soft-core extended Hubbard models by using the Gutzwiller variational wave function. Contrary to previous studies, we adopted a canonical ensemble and a linear programming method, to more directly include phase separations in our calculations. In the hard-core model, away from the half filling, we showed that the SF phase splits into the SF and solid phases at a critical value of the nearest-neighbor interaction V that agrees with a perturbative

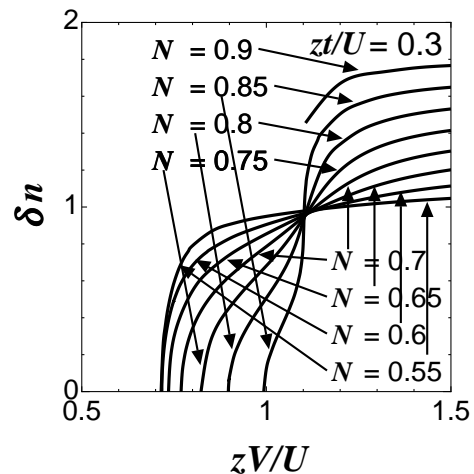


FIG. 9: Nearest-neighbor interaction dependence of $\delta n = |N_A - N_B|$ of the soft-core model for $zt/U = 0.3$ above half filling. For small zt/U , δn is larger at smaller N ; however, for large zt/U , δn is smaller at smaller N . Contrary to the case of $zt/U = 0.03$ (Fig. 7), δn is a continuous function of zV/U , except for $N = 0.9$ where $\delta n = 0$ for small $zt/U \leq 1.105$ (The phase is SF there).

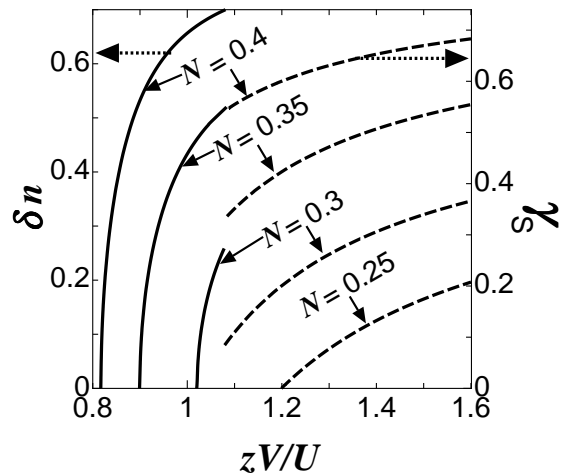


FIG. 10: Nearest-neighbor interaction dependences of $\delta n = |N_A - N_B|$ and γ_S of the soft-core model for $zt/U = 0.3$ below half-filling shown by the solid and dashed curves, respectively. For $N = 0.3, 0.35$, and 0.4 , $\gamma_S(\delta n)$ is zero below (above) the critical value of zV/U for the SF-PS(SF+S) transition and discontinuously becomes finite above (below) the critical value. In contrast, $\delta n = 0$ for $N = 0.25$ in the entire figure because the SS phase does not exist.

calculation.

Contrary to the hard-core model, the soft-core model at half filling has a possible SS phase between the solid and SF phases and all the phase transitions are continuous.

Away from half filling, the phase diagram drastically depends on the transfer integral t . For small zt/U , the shape of the SF region is similar to that of the hard-core

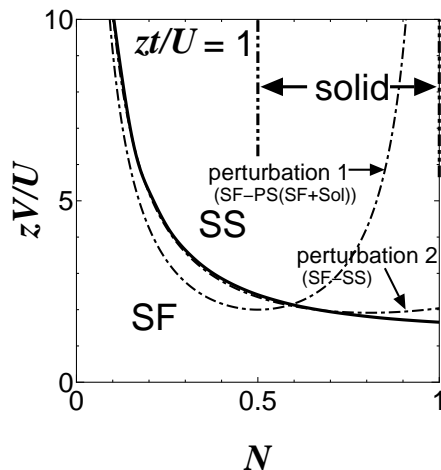


FIG. 11: Phase diagram of the soft-core model for $zt/U = 1$. The solid curve shows the SF–SS phase boundary where the phase transition is continuous. The dot-dashed curves show the results of perturbation 1 (Eq. 9) and 2 (Eq. B16). The two-dot-dashed lines at half filling and unit filling show the solid phases.

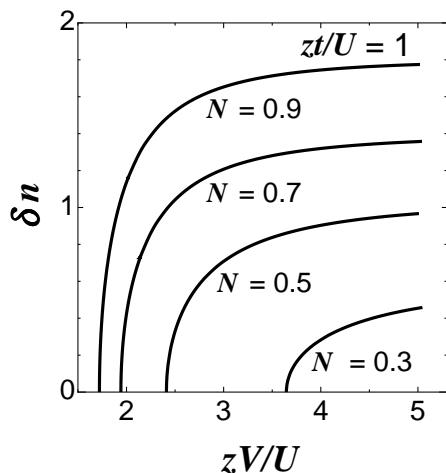


FIG. 12: Nearest-neighbor interaction dependence of $\delta n = |N_A - N_B|$ of the soft-core model at $N = 0.3, 0.5, 0.7,$ and 0.9 for $zt/U = 1$.

model. The separated phase with the SF and the $N = 1/2$ solid phases appears below half filling and the SS phase appears only above half filling, as in the 2D QMC studies. For intermediate zt/U , the SS phase appears close to the separated phase below half filling as in the 3D QMC study. The phase diagram gets simplified for large zt/U , where there is only the continuous SF–SS phase transition and the critical value of zV/U at the phase boundary is a smooth decreasing function of N .

The nearest-neighbor interaction dependence of $\delta n = |N_A - N_B|$, which shows the density wave order of the SS phase, is also interesting. For a small zt/U of 0.03, δn is a discontinuous function of zV/U ; further, the SS

phase has small δn for small $zV/U < 1$ and large $\delta n \simeq 2N$ ($N_A \simeq 2N$ and $N_B \simeq 0$) for large $zV/U > 1$. In addition, δn is larger for smaller (larger) N for small $zV/U < 1$ (large $zV/U > 1$). For an intermediate zt/U of 0.3, the behavior of δn is similar to that in the case of $zt/U = 0.03$. However, contrary to the case of $zt/U = 0.03$, the two curves of δn for two different N intersect around $zV/U \simeq 1$ because δn is a continuous increasing function of zV/U . For a large $zt/U = 0.1$, δn is a smooth increasing function of N and zV/U , and the two curves of δn for two different N s no longer intersect.

Throughout this paper, we found that our perturbative calculations excellently determined the phase boundary curves, except for large $N \sim 1$.

Because the Gutzwiller approximation is not exact, exact numerical calculations such as QMC are needed to check our results; however, these exact calculations should assume the possible phase separations as performed in this paper. Although some details (such as very complicated phase diagrams for large N and small zt) might be artifacts of our approximation, we believe that the important results from the phase diagrams and δn in the SS phase are worth checking. For instance, the transfer integral dependence of the whole phase diagram seems to remain an open question not only in 3D but also in 2D, especially for the large zt/U regime where a SS phase below half filling might exist.

Appendix A: PERTURBATIVE CALCULATIONS FOR THE HARD-CORE MODEL

1. THE SF–SS TRANSITION

In the Gutzwiller approximation, the energy expectation value of the Hamiltonian (Eq. 1) is obtained as

$$\begin{aligned} E &= E_{\text{kin}} + E_{\text{int}}^V, \\ E_{\text{kin}} &= -zt c_{A0} c_{B0} c_{A1} c_{B1}, \\ E_{\text{int}}^V &= \frac{zV}{2} c_{A1}^2 c_{B1}^2. \end{aligned} \quad (\text{A1})$$

Here, we assumed $c_{A(B)n}$ ($n = 0, 1$) is real without the loss of generality and used $\langle a_{A(B)} \rangle = c_{A(B)0} c_{A(B)1}$ and $\langle a_{A(B)}^\dagger a_{A(B)} \rangle = c_{A(B)1}^2$. To consider the SS phase that is infinitesimally close to the SF–SS phase boundary, we set $c_{A(B)n} = c_n + \delta\alpha_n + i\delta\beta_n$, where $\delta\alpha_n$ and $\delta\beta_n$ are infinitesimal quantities. The normalization condition of the wave function for sublattices A and B is written as

$$\begin{aligned} (c_0 + \delta\alpha_0)^2 + (c_1 + \delta\alpha_1)^2 &= 1, \\ (c_0 + \delta\beta_0)^2 + (c_1 + \delta\beta_1)^2 &= 1. \end{aligned} \quad (\text{A2})$$

The boson number condition is written as

$$(c_1 + \delta\alpha_1)^2 + (c_1 + \delta\beta_1)^2 = 2N. \quad (\text{A3})$$

These equations can be rewritten by using the normalization and boson number conditions in the SF phase

($\sum_n c_n^2 = 1$ and $\sum_n n c_n^2 = N$, respectively) as

$$\begin{aligned} 4c_0\delta x_0 + \delta x_0^2 + \delta y_0^2 &= 0, \\ 4c_1\delta x_1 + \delta x_1^2 + \delta y_1^2 &= 0, \\ c_0\delta y_0 + c_1\delta y_1 + \delta x_0\delta y_0 &= 0. \end{aligned} \quad (\text{A4})$$

Here, we introduced new variables $\delta x_n(\delta y_n) = \delta\alpha_n + (-)\delta\beta_n$ and $\delta y_n \neq 0$. These equations can be further rewritten in the lowest order as

$$\begin{aligned} 4c_0\delta x_0 + \delta y_0^2 &= 0, \\ 4c_1\delta x_1 + \delta y_1^2 &= 0, \\ 2c_0\delta y_0 + 2c_1\delta y_1 &= 0. \end{aligned} \quad (\text{A5})$$

Hence, δx_n are of the same order as δy_n^2 and δx_n can be rewritten in terms of δy_n . Then, the energy expectation values can also be rewritten in terms of δy_n as

$$\begin{aligned} E_{\text{kin}} &= -zt \left[N(1-N) - \frac{1}{2}(1-N)\delta y_1^2 - \frac{1}{2}N\delta y_0^2 \right], \\ E_{\text{int}}^V &= \frac{zV}{2} \left[N^2 - N\delta y_1^2 \right]. \end{aligned} \quad (\text{A6})$$

Therefore,

$$\begin{aligned} E &= -zt N(1-N) + \frac{zt}{2}N^2 \\ &\quad + \frac{1}{2} \left[zt \frac{N^2 + (1-N)^2}{1-N} - zVN \right] \delta y_1^2. \end{aligned} \quad (\text{A7})$$

By equating the coefficient of δy to zero, we obtain the critical value of V for the SF-SS transition (Eq. 9).

2. THE PHASE SEPARATION INTO THE SS AND SOLID PHASES

To obtain the phase boundary, we substitute Eq. 11 into Eq. 12. The result is

$$\begin{aligned} E &= -zt N(1-N) + \frac{zV}{2}N^2 \\ &\quad + \left\{ ztN^2 + \frac{zV}{2}N^2 + E_{\text{SM}} \right. \\ &\quad \left. + [-zVN + zt(1-2N)]N_{\text{SM}} \right\} \gamma_{\text{SM}}. \end{aligned} \quad (\text{A8})$$

In the case of the phase separation that split into the SF and solid phases, $N_{\text{SM}} = 1/2$ and $E_{\text{SM}} = 0$ and by equating the coefficient of γ_{SM} to zero, we obtain the critical value of V for the phase separation (Eq. 9). In contrast, the MI phase has $N_{\text{SM}} = 1/2$ and $E_{\text{SM}} = zV/2$ and the coefficient of γ_{SM} is positive definite:

$$zt(N-1)^2 + \frac{zV}{2}(N^2 - N + 1) > 0. \quad (\text{A9})$$

Hence, phase separation into the SF and MI phases does not occur.

Appendix B: PERTURBATIVE CALCULATIONS FOR THE SOFT-CORE MODEL

1. THE SS-SOLID TRANSITION

To obtain the SS-solid phase boundary (Eq. 13), we set $c_{A0} = \delta\alpha_0$, $c_{A1} = 1 - \delta\alpha_1$, $c_{A2} = \delta\alpha_2$, $c_{B0} = 1 - \delta\beta_0$, $c_{B1} = \delta\beta_1$, and $c_{B2} = \delta\beta_2$. The normalization conditions for sublattices A and B lead to the following equations in the lowest order:

$$\begin{aligned} \delta\alpha_1 &= \frac{1}{2}(\delta\alpha_0^2 + \delta\alpha_2^2), \\ \delta\beta_0 &= \frac{1}{2}(\delta\beta_1^2 + \delta\beta_2^2). \end{aligned} \quad (\text{B1})$$

In addition, the boson number condition leads to

$$\delta\alpha_1 = \delta\alpha_2^2 + \frac{1}{2}\delta\beta_1^2 + \delta\beta_2^2. \quad (\text{B2})$$

From these equations, we can eliminate $\delta\alpha_0$, $\delta\alpha_1$, and $\delta\beta_0$ and obtain the energy in terms of $\delta\alpha_2$, $\delta\beta_1$, and $\delta\beta_2$ as

$$\begin{aligned} E &= \frac{U}{2}\delta\alpha_2^2 + \frac{zV}{2}\delta\beta_1^2 + \left(\frac{U}{2} + zV \right) \delta\beta_2^2 \\ &\quad - zt \left(\sqrt{2}\delta\alpha_2 + \sqrt{\delta\alpha_2^2 + \delta\beta_1^2 + 2\delta\beta_2^2} \right) \delta\beta_1 \\ &= \left[\frac{U}{2}x^2 + \frac{zV}{2} + \left(\frac{U}{2} + zV \right) y^2 \right. \\ &\quad \left. - zt \left(\sqrt{2}x + \sqrt{1+x^2+2y^2} \right) \right] \delta\beta_1^2, \end{aligned} \quad (\text{B3})$$

where we have set $\delta\alpha_2 = x\delta\beta_1$ and $\delta\beta_2 = y\delta\beta_1$. The minimization conditions of Eq. B3 are written as

$$\frac{1}{\delta\beta_1^2} \frac{\partial E}{\partial x} = Ux - \sqrt{2}zt - \frac{zt x}{\sqrt{1+x^2+2y^2}} = 0, \quad (\text{B4})$$

$$\frac{1}{\delta\beta_1^2} \frac{\partial E}{\partial y} = (U + 2zV)y - \frac{2zty}{\sqrt{1+x^2+2y^2}} = 0. \quad (\text{B5})$$

The latter equation leads to $y = 0$ because we assume small $zt (< U)$. From the former equation, we have

$$x = \frac{\sqrt{2}zt}{U} \left(1 + \frac{zt}{U} \right) + O\left(\frac{z^3 t^3}{U^3} \right). \quad (\text{B6})$$

By substituting the x obtained above into Eq. B3, we obtain the critical value of zV for the SS-solid phase transition (Eq. 13).

2. THE SF-SS TRANSITION

As explained in the text, we limit the Hilbert space to three states $|0\rangle$, $|1\rangle$, and $|2\rangle$. Furthermore, we set $c_{An} = c_n + \delta\alpha_n$ and $c_{Bn} = c_n + \delta\beta_n$ where $\delta\alpha_n$ and $\delta\beta_n$ ($n = 0, 1, 2$) are infinitesimal quantities. We determine c_n ($n = 0, 1, 2$) to minimize the energy of the SF phase.

As in the case of the hard-core model (Appendix A.1), we introduce δx_n (δy_n) = $\delta\alpha_n$ + $(-)\delta\beta_n$, where $\delta y_n \neq 0$ for the SS phase. The normalization condition of the wave function and the boson number condition lead to

$$\begin{aligned} c_0\delta x_0 + c_1\delta x_1 + c_2\delta x_2 &= -\frac{1}{4}(\delta y_0^2 + \delta y_1^2 + \delta y_2^2), \\ 2c_1\delta x_1 + 4c_2\delta x_2 &= -\frac{\delta y_1^2}{2} - \delta y_2^2, \\ c_0\delta y_0 + c_1\delta y_1 + c_2\delta y_2 &= 0 \end{aligned} \quad (\text{B7})$$

in the lowest order of δx_n and δy_n (δx_n are of the order of δy_n^2). By eliminating δx_0 , δx_1 , and δy_1 in the above equations, the energy per site is written in terms of δx_2 , δy_0 , and δy_2 as

$$\begin{aligned} E &= E_{\text{kin}} + E_{\text{int}}^U + E_{\text{int}}^V, \\ E_{\text{kin}} &= -zt \left[c_1^2 (\sqrt{2}c_2 + c_0)^2 + X\delta x_2 \right. \\ &\quad \left. - \frac{1}{4}(a_0\delta y_0^2 + a_{02}\delta y_0\delta y_2 + a_2\delta y_2^2) \right], \\ E_{\text{int}}^U &= U \left[c_2^2 + c_2\delta x_2 + \frac{1}{4}\delta y_2^2 \right], \\ E_{\text{int}}^V &= \frac{zV}{2} \left[(c_1^2 + 2c_2^2)^2 - (c_0\delta y_0 - c_2\delta y_2)^2 \right], \end{aligned} \quad (\text{B8})$$

where

$$\begin{aligned} X &= (\sqrt{2}c_2 + c_0) \left[c_1^2 \left(\sqrt{2} + \frac{c_2}{c_0} \right) \right. \\ &\quad \left. - 2c_2(\sqrt{2}c_2 + c_0) \right], \end{aligned} \quad (\text{B9})$$

$$a_0 = \left(2 + \frac{\sqrt{2}c_2}{c_0} \right) c_1^2 + \frac{2c_0^2}{c_1^2} (\sqrt{2}c_2 + c_0)^2, \quad (\text{B10})$$

$$a_{02} = 2 \left[\sqrt{2}c_1^2 + \frac{2c_0c_2}{c_1^2} (\sqrt{2}c_2 + c_0)^2 \right], \quad (\text{B11})$$

$$\begin{aligned} a_2 &= 2(\sqrt{2}c_2 + c_0)^2 \left(1 + \frac{c_2^2}{c_1^2} \right) \\ &\quad + c_1^2 \left(1 - \frac{\sqrt{2}c_2}{c_0} \right). \end{aligned} \quad (\text{B12})$$

The total coefficient of δx_2 in E of Eq. B8 is zero, because the variation of δx_n corresponds to the variation of c_n in the SF phase, and the values of c_n were already determined to minimize E . To be concrete, the energy of the SF phase is written by c_2 when $\delta y_n = 0$ as

$$\begin{aligned} E_{\text{SF}} &= -zt(N - 2c_2^2) \left(\sqrt{2}c_2 + \sqrt{1 - N + c_2^2} \right)^2 \\ &\quad + \frac{zV}{2} N^2 + Uc_2^2, \end{aligned} \quad (\text{B13})$$

where c_0 and c_1 were already eliminated by the normalization and boson number conditions. The minimization condition $\frac{dE_{\text{SF}}}{dc_2} = 0$ leads to

$$\begin{aligned} Uc_2 &= zt \left[c_2 \left(\sqrt{2}c_2 + \sqrt{1 - N + c_2^2} \right)^2 \right. \\ &\quad \left. + \frac{(N - 2c_2^2) \left(\sqrt{2}c_2 + \sqrt{1 - N + c_2^2} \right) \left(c_2 + \sqrt{2(1 - N + c_2^2)} \right)}{\sqrt{1 - N + c_2^2}} \right] \end{aligned} \quad (\text{B14})$$

and we can easily verify that the total coefficient of δx_2 in E of Eq. B8 is zero by using Eq. B14.

E is further rewritten as

$$\begin{aligned} E &= \text{const.} + A\delta y_0^2 + B\delta y_0\delta y_2 + C\delta y_2^2, \\ A &= \frac{zt}{4}a_0 - \frac{zV}{2}c_0^2, \\ B &= \frac{zt}{4}a_{02} + zVc_0c_2, \\ C &= \frac{zt}{4}a_2 - \frac{zV}{2}c_2^2 + \frac{U}{4}. \end{aligned} \quad (\text{B15})$$

Hence, δy_n becomes finite when $B^2 > 4AC$, which corresponds to $V > V_C^{\text{SF-SS}}$, where

$$V_C^{\text{SF-SS}} = \frac{t}{8} \frac{zt(4a_0a_2 - a_{02}^2) + 4Ua_0}{zt(c_2^2a_0 + c_0c_2a_{02} + c_0^2a_2) + Uc_0^2}. \quad (\text{B16})$$

To obtain the numerical value of Eq. B16, we numerically find the value of c_2 that minimizes E (Eq. B13). On the other hand, to obtain the critical value of V for the SF-SS transition at half filling (Eq. 14), we start from the minimization condition obtained from Eq. B13 up to the second order of c_2 :

$$\frac{dE}{dc_2} = -zt(1 + c_2 - 9c_2^2) + 2Uc_2 = 0. \quad (\text{B17})$$

By setting $c_2 = azt/U + bz^2t^2/U^2$ in the above equation, we obtain $c_2 = zt/(2U) + z^2t^2/(4U^2)$. Now, a_0 , a_{02} , and a_2 are written as

$$\begin{aligned} a_0 &= 2 + 5\delta + 13\delta^2, \\ a_{02} &= \sqrt{2}(1 + 2\delta + 6\delta^2), \\ a_2 &= \frac{3}{2}(1 + 2\delta + 6\delta^2), \end{aligned} \quad (\text{B18})$$

where $\delta = zt/(2U)$. By substituting a_0 , a_{02} , and a_2 into Eq. B16, we obtain the critical value of V (Eq. 14).

3. THE PHASE SEPARATION INTO THE SF AND SOLID PHASES

As explained in the text and in Appendix B. 2, we limit the Hilbert space to three states: $|0\rangle$, $|1\rangle$, and $|2\rangle$. We assume that c_n (where $n = 0, 1, 2$) is determined to minimize the total energy of the SF phase (not the separated phase). The normalization and boson number conditions are written as $\sum_n c_n^2 = 1$ and $\sum_n nc_n^2 = N$, respectively. We set $c_i \rightarrow c_n + \delta c_n$ and $N \rightarrow N - \delta N$ for the SF phase in the separated phase and γ_{SM} as the ratio of the solid (MI) phase to the whole system. The boson number condition in the entire system is written as $\delta N = \gamma_{\text{SM}}(N_{\text{SM}} - N)$ in the lowest orders of γ_{SM} and δN , where we assume $N_{\text{SM}} = 1/2$ or 1 for the solid phase or $N_{\text{SM}} = 1$ for the MI phase, respectively, because we assume $N \leq 1$. The normalization and boson number conditions for the SF phase in the separated phase are written as $\sum_n (c_n + \delta c_n)^2 = 1$ and $\sum_n n(c_n + \delta c_n)^2 = N - \delta N$, respectively. These equations are rewritten as

$$\begin{aligned} \delta c_0 &= -\frac{1}{4c_0} (2c_1\delta c_1 - \delta N), \\ \delta c_2 &= -\frac{1}{4c_2} (2c_1\delta c_1 + \delta N). \end{aligned} \quad (\text{B19})$$

From these equations and the minimization condition for E_{SF} (Eq. B14), we determine the energy of the SF phase E_{SF} in the separated phase as

$$E_{\text{SF}} = -zt(N - 2c_2^2)\left(\sqrt{2}c_2 + \sqrt{1 - N + c_2^2}\right)^2 + \frac{zV}{2}N^2 + Uc_2^2 + Y\delta N, \quad (\text{B20})$$

where

$$Y = -\frac{zt}{2}c_1^2(\sqrt{2}c_2 + c_0)\left(-\frac{\sqrt{2}}{c_2} + \frac{1}{c_0}\right) - zVN - \frac{U}{2}. \quad (\text{B21})$$

Note that the δc_1 term is eliminated because to Eq. B14. Because the ratio of the SF phase in the separated phase is $1 - \gamma_{\text{SM}}$ and $\gamma_{\text{SM}}(N_{\text{SM}} - N) = \delta N$, the energy of the entire system E is written as

$$E = -zt(N - 2c_2^2)\left(\sqrt{2}c_2 + \sqrt{1 - N + c_2^2}\right)^2 + \frac{zV}{2}N^2 + Uc_2^2 + (Azt - BzV - CU + E_{\text{SM}})\gamma_{\text{SM}}, \quad (\text{B22})$$

where

$$\begin{aligned} A &= c_1^2\left[(\sqrt{2}c_2 + c_0)^2 + \frac{1}{2}\left(1 + \sqrt{2}\frac{c_0^2 - c_2^2}{c_0c_2}\right)(N_{\text{SM}} - N)\right], \\ B &= N\left(N_{\text{SM}} - \frac{N}{2}\right), \\ C &= c_2^2 + \frac{1}{2}(N_{\text{SM}} - N) \end{aligned} \quad (\text{B23})$$

and E_{SM} is the energy of the solid (MI) phase. In particular, $E_{\text{SM}} = 0$ ($E_{\text{SM}} = U/2$) for the solid phase with $N = 1/2$ ($N = 1$) and $E_{\text{SM}} = zV$ for the MI phase.

Finally, equating the coefficient of γ_{SM} to zero, we find that the critical value of the SF-PS transition is

$$V_C^{\text{SF-PS(SF+S)}} = \frac{zA - UC + E_{\text{SM}}}{zB}. \quad (\text{B24})$$

-
- [1] A.F. Andreev and I.M. Lifshitz, Zh. Eksp. i. Teor. Fiz. **56**, 2057 (1969); Soviet Phys. JETP **29**, 1107 (1969).
[2] G.V. Chester, Phys. Rev. A **2**, 256 (1970).
[3] A.J. Leggett, Phys. Rev. Lett. **25**, 1543 (1970).
[4] E. Kim and M. Chan, Nature (London) **427**, 225 (2004).
[5] M.P.A. Fisher, P.B. Weichman, G. Grinstein, and D.S. Fisher, Phys. Rev. B **40**, 546 (1989).
[6] D. Jaksch, C. Bruder, J.I. Cirac, C.W. Gardiner, and P. Zoller, Phys. Rev. Lett. **81**, 3108 (1998).
[7] M. Greiner, O. Mandel, T. Esslinger, T.W. Hansch, and I. Bloch, Nature **415**, 918 (2002).
[8] A. Griesmaier, J. Werner, S. Hensler, J. Stuhler, and T. Pfau, Phys. Rev. Lett. **94**, 160401 (2005).
[9] H. Matsuda and T. Tsuneto, Suppl. Prog. Theor. Phys. **16**, 569 (1970).
[10] M. Iskin and J.K. Freericks, Phys. Rev. A **79**, 053634 (2009).
[11] J.K. Freericks and H. Monien, Europhys. Lett. **26**, 545 (1994).
[12] J.K. Freericks and H. Monien, Phys. Rev. B **53**, 2691 (1996).
[13] R.T. Scalettar, G.G. Batrouni, and G.T. Zimanyi, Phys. Rev. Lett. **66**, 3144 (1991).
[14] P. Niyaz, R.T. Scalettar, C.Y. Fong, and G.G. Batrouni, Phys. Rev. B **44**, 7143 (1991).
[15] G.G. Batrouni and R.T. Scalettar, Phys. Rev. B. **46**, 9051 (1992).
[16] A. van Otterlo and K.-H. Wagenblast, Phys. Rev. Lett. **72**, 3598 (1994).
[17] B. Capogrosso-Sansone, N.V. Prokof'ev, and B.V. Svistunov, Phys. Rev. B **75**, 134302 (2007).
[18] B. Capogrosso-Sansone, S.G. Söyler, N.V. Prokof'ev, and B.V. Svistunov, Phys. Rev. A **77**, 015602 (2008).
[19] D.S. Rokhsar and B.G. Kotliar, Phys. Rev. B **44**, 10328 (1991).
[20] W. Krauth, M. Caffarel and J.-P. Bouchaud, Phys. Rev. B **45**, 3137 (1992).
[21] T. Kimura, S. Tsuchiya, and S. Kurihara, Phys. Rev. Lett. **94**, 110403 (2005).
[22] T. Kimura, S. Tsuchiya, M. Yamashita, and S. Kurihara, J. Phys. Soc. Jpn. **75**, 074601 (2006).
[23] K.V. Krutitsky and R. Graham, Phys. Rev. A **70**, 063610 (2004).
[24] K.-S. Liu and M.E. Fisher, J. Low Temp. Phys. **10**, 655 (1973).
[25] C. Bruder, R. Fazio, and G. Schön, Phys. Rev. B **47**, 342 (1993).
[26] R.T. Scalettar, G.G. Batrouni, A.P. Kampf, and G.T. Zimanyi, Phys. Rev. B **51**, 8467 (1995).
[27] G.G. Batrouni, R.T. Scalettar, G.T. Zimanyi, and A.P. Kampf, Phys. Rev. Lett. **74**, 2527 (1995).
[28] G.G. Batrouni and R.T. Scalettar, Phys. Rev. Lett. **84**, 1599 (2000).
[29] F. Hébert, G.G. Batrouni, R.T. Scalettar, G. Schmid, M. Troyer, and A. Dorneich Phys. Rev. B **65**, 014513 (2001).
[30] A. van Otterlo, K.-H. Wagenblast, R. Baltin, C. Bruder, R. Fazio, and G. Schön, Phys. Rev. B **52**, 16176 (1995).
[31] V.W. Scarola, E. Demler, and S. Das Sarma, Phys. Rev. A **73**, 051601(R) 2006.
[32] P. Sengupta, L.P. Pryadko, F. Alet, M. Troyer, and G. Schmid, Phys. Rev. Lett. **94**, 207202 (2005).
[33] F. Hébert, G.G. Batrouni and R.T. Scalettar, Phys. Rev. A **71**, 063609 (2005),
[34] G.G. Batrouni, F. Hébert, and R.T. Scalettar, Phys. Rev. Lett. **97**, 087209 (2006).
[35] T.D. Kühner and H. Monien, Phys. Rev. B **58**, R14741 (1998).
[36] T.D. Kühner, S.R. White, and H. Monien, Phys. Rev. B **61**, 12474 (2000).
[37] T. Mishra, R.V. Pai, S. Ramanan, M.S. Luthra, and B.P.

- Das, Phys. Rev. A **80**, 043614 (2009).
- [38] K. Yamamoto, S. Todo, and S. Miyashita, Phys. Rev. B **79**, 094503 (2009).
- [39] W.H. Press, S.A. Teukolsky, and W.T. Vetterling, *Numerical Recipes in Fortran: The Art of Scientific Computing*, Cambridge Univ. (1992).
- [40] Though we tried to directly impose the direct boson number condition $\sum_n n|c(n)|^2 = N_{\text{SF}}$ on the wave function in addition to the normalization condition $\sum_n |c(n)|^2 = 1$, convergence of the calculation was poor compared to the method explained in the text.
- [41] P. Nozières, J. Low Temp. Phys. **137**, 45 (2004).